J. Anat. (1984), **139**, 2, pp. 275–294
With 13 *figures*
Printed in Great Britain

Further insights into the structural principles governing the function of articular cartilage

NEIL D. BROOM

Department of Mechanical Engineering, University of Auckland
Private Bag, Auckland, New Zealand

(*Accepted* 12 *January* 1984)

INTRODUCTION

The compressive load-bearing properties of articular cartilage arise principally from the interplay between the collagen fibres and the hydrated proteoglycan complexes. The tension supporting fibres are arranged in a three dimensional interconnecting meshwork and the highly deformable hydrated proteoglycan molecules swell out within this constraining structure (Meachim & Stockwell, 1979). Together these primary components result in a composite structure capable of sustaining the full range of loading patterns transmitted through the articulating joint.

Degenerative changes affecting the mechanical function of articular cartilage are manifested as an alteration in the integrity of either or both of these components and their relationship to each other. As in any composite material, it is often difficult to assess experimentally the contribution each component makes to the overall functional performance of the material; the ultrastructural scale of size of the components in articular cartilage contributes substantially to this problem.

Compression data from bulk samples of cartilage are plentiful (Weightman & Kempson, 1979) and more recently the present author has used a combination of microcompression and differential interference contrast to examine the structural response to load of fresh samples of this tissue (Broom & Myers, 1980; Broom & Poole, 1982; Broom, 1982; Broom & Poole, 1983).

What is still needed however is a method of obtaining at a local microscopic level accurate mechanical/structural correlations throughout the various functional zones of cartilage. Such an approach should yield a more complete understanding of the subtle interplay between the primary components of this important tissue which give rise to both normal and abnormal function.

In this paper a new experimental approach is used to make such an assessment of fresh articular cartilage. A technique is employed involving observation by differential interference microscopy of the propagation of an artificially induced notch in this tissue.

The results obtained provide substantial experimental support for the structural model proposed recently by the author (Broom, 1982) and extend current knowledge of the structural principles governing the biomechanical function of articular cartilage.

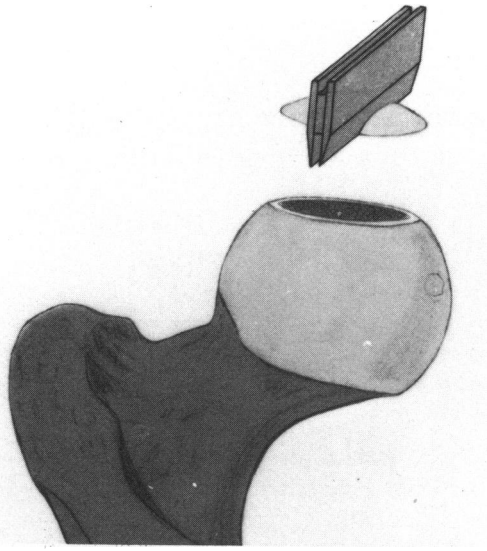

Fig. 1. Schematic diagram demonstrating cutting technique used to obtain full thickness slices of fresh articular cartilage from a joint surface. The actual tissue used in the present study was from the lower end of femur and from the tibial surface – not the head of femur as implied from this schematic picture.

EXPERIMENTAL METHODS

Full depth scallops of normal bovine articular cartilage 1·2–2·4 mm in thickness were removed from femoral patellar surfaces of freshly slaughtered prime oxen (two to three years old). Scallops of softened cartilage 2·1–3·0 mm thick were also taken from central tibial condylar surfaces. The biomechanical condition of the cartilage from these two different sites was initially assessed using methods previously described (Broom, 1982). A cutting technique, shown schematically in Figure 1, provided full depth slices of tissue 0·1–0·2 mm in thickness from the scallops. The femoral patellar slices were taken in the anterior–posterior plane of orientation and the tibial slices from random orientations. A sharp scalpel was then used to notch these slices either radially from the articular surface cutting down into the underlying matrix to approximately half the full depth of the cartilage thickness (Fig. 2*a*) or transversely at the same depth cutting parallel to the articular surface (Fig. 2*b*). The slices were mounted in a microtensile device which was inserted directly onto the stage of an optical microscope equipped with Nomarski differential interference contrast. The interference contrast system of imaging exploits differences in optical density of the various components of the tissue in order to achieve contrast (Phillips, 1971). Structural features such as chondrocytes and aggregates of fibres are easily resolved at any given focal plane in the fresh unstained cartilage. The experimental procedures are fully described in previous work by the present author (Broom, 1978; Broom & Myers, 1980). The loading patterns for the radially and transversely notched slices are also shown schematically in Figure 2. Continuous load–crosshead extension curves were obtained from the notch propagation tests and plotted with an x–y chart recorder. A crosshead speed of 0·75 mm per minute was used in all tests. Because of the geometry of the notched specimens, normalised stress/strain curves could not be obtained from the tissue loading experiments: the load–extension curves

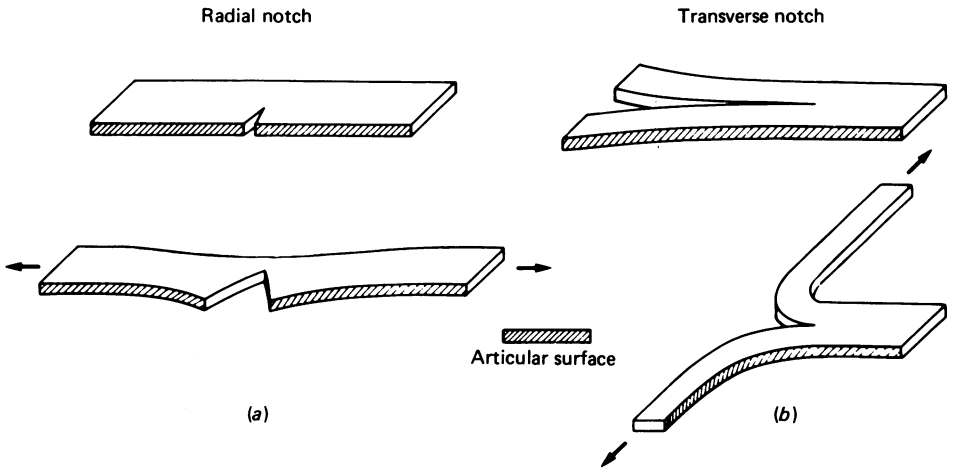

Fig. 2 (*a–b*). Schematic diagram showing radial (*a*) and transverse (*b*) notch geometries and their respective loading configurations.

obtained were solely a means of monitoring in each slice the load required for notch propagation. Slices of identical thickness were used when comparing loads required for propagation in different tissue types or notch directions. More than 100 slices from 36 different scallops of cartilage were examined.

RESULTS

The bulk scallops of fresh macroscopically normal articular cartilage from the patellar groove region, when released from their subchondral bone, exhibited highly variable shape characteristics. Some scallops rapidly curled upwards to varying degrees to enclose the articular surface – indicating a significant relaxation of strain within the cartilage matrix (Fry, 1974). Others underwent little or no change from that of their *in situ* aspect and were noticeably smaller in their surface-to-deep or radial dimension than the curled scallops. Scallops from the softened tibial condylar surfaces always contracted upwards to enclose the articular surface and were larger in their radial dimension than either of the above. For the purpose of the present study it was convenient to categorise the tightly contracted normal patellar groove scallops as type A, those exhibiting negligible relaxation as type B, and scallops from the softened tibial condylar surfaces as type C.

Load–extension studies of intact slices

Preliminary tensile loading of intact type A and B slices confirmed that the superficial layer of cartilage had a dominant role in determining their initial mechanical response. The continuous loading curve for type A slices (Fig. 3) was always interrupted by a single radial crack initiated in this superficial layer. The instantaneous large reduction in load was followed by a slight increase in load as the radial cleft continued to propagate radially through the entire width of the slice. In type B slices (Fig. 3), higher load levels were reached before a single crack was initiated again in the superficial layer with only a slight instantaneous reduction in load. This was followed by a fairly rapid increase in load as this single crack encountered increasing resistance to radial propagation. A second crack then developed at some other site

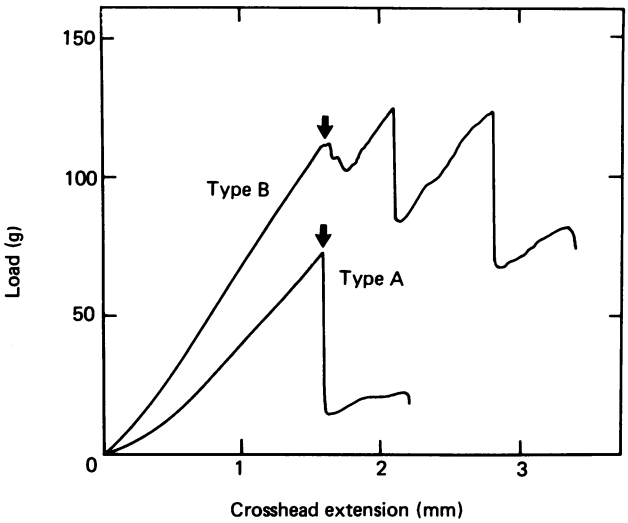

Fig. 3. Load–extension curves for un-notched type A and type B slices. Arrows indicate load reached at initiation of crack in superficial layer.

on the articular surface and the whole process repeated several times, thus resulting in a 'saw-tooth' mechanical response. Eventual failure of the slices was a consequence of the preferential propagation of just one of these cracks.

The type C slices were structurally so weak that radial cracks, often pre-existing in the superficial layer, propagated at negligible tensile loads (see below).

Load–extension studies of prenotched slices

Radially notched slices

Representative tensile load–extension curves for type A and B slices are shown in Figure 4. The first indication of tearing at the notch root is shown on each curve. The curves demonstrate the markedly different loading levels required to propagate a radial notch through the deep matrix of these two categories of tissue. Both slices were of similar gauge length so that the curves also indicate the difference in stiffness between these two categories. The load–extension curve for a radially notched, type C slice is also shown in Figure 4 in order to demonstrate its greatly reduced strength relative to type A and B tissues.

Transversely notched slices

The general pattern of mechanical response in the transversely notched type A and B slices was similar. Figure 5 shows load–extension curves for a transversely notched type B slice and a radially notched adjacent slice from the same scallop to permit direct comparison of the two different notch configurations.

The onset of tearing at the transverse notch root always occurred at a lower load than that at the radial notch root. Furthermore, the load–extension curve for the transverse notched slice consistently exhibited two or three distinct regimes of response which were related directly to the pathway of tissue tearing. The first regime covered the initial stage of loading up to the first indication of tearing at the notch root. The second commenced with the almost immediate deflection of the transverse notch towards a generally radial direction either down into the deeper matrix, with

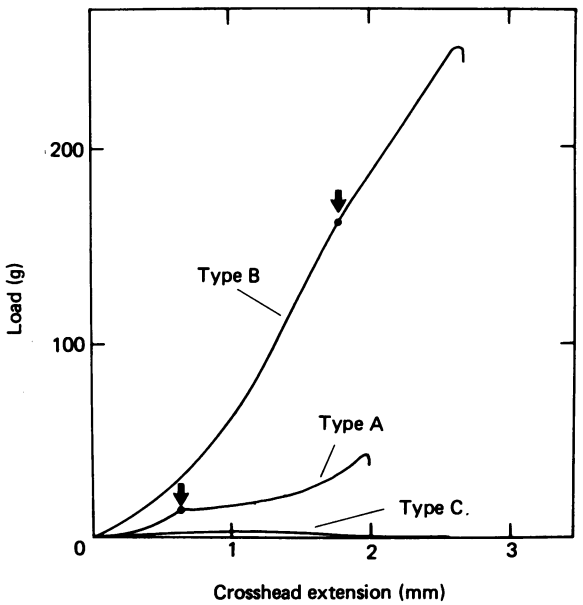

Fig. 4. Load–extension curves for radially notched type A, B and C slices. Arrows indicate load at onset of tearing at notch root in type A and B slices.

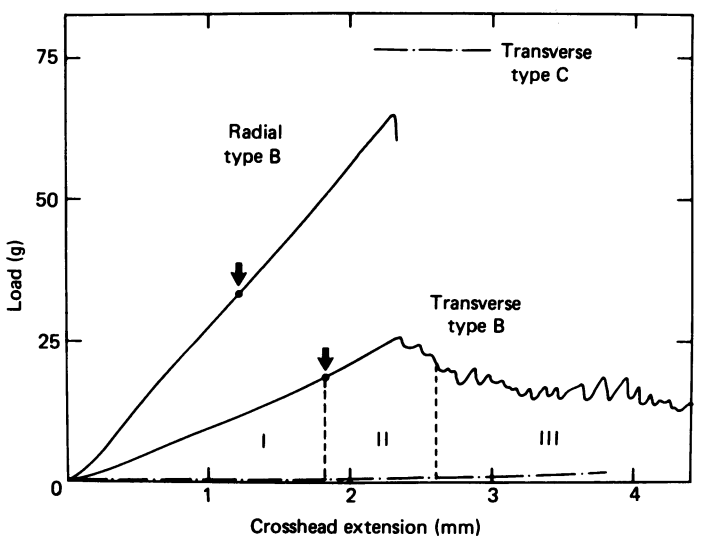

Fig. 5. Load–extension curves for identical type B slices, radially and transversely notched. Loading regimes I, II and III are indicated on the transverse curve. A type C response is also shown for comparison. Arrows indicate load at onset of tearing.

increasing load proceeding to final failure, or up towards the superficial zone. When this latter upward radial deflection occurred, a third regime was observed during which the load dropped and the secondary radial notch again reverted to a transverse mode propagating parallel to the articular surface but at a consistently observed depth of about 150 μm. This final regime involved in effect a delamination mechanism and proceeded at a relatively uniform load until the entire surface of the cartilage

was detached. No fracture in tension of this superficial layer was ever observed during this delamination stage.

The response of a transversely notched type C slice is also indicated in Figure 5. The very small loads at which tearing occurred always involved an immediate radial deflection of the notch. Final failure often occurred at sites other than in the vicinity of the original notch.

Interference light microscopy

General

With particular reference to the deep zone in each of the three types of tissue a consistent pattern of matrix textures was observed. A fine but pronounced radial texture was present in type A tissue (Fig. 6*a*) but not in type B (Fig. 6*b*). Type C tissue exhibited a clearly resolved radial texture consisting of straight or crimped fibrous bundles (Fig. 6*c*).

The polarised illumination conditions required to obtain differential interference contrast imaging of the fine structure of the fresh articular cartilage also provided a qualitative indication of stress concentration within the tissue. Under load, regions of highest stress darkened relative to the surrounding matrix thus aiding the biomechanical interpretation.*

Radial notch propagation

Type A tissue. The propagation of a radial notch is shown in Figure 7. The sharp notch (Fig.7*a*) extended well into the deep zone of the unloaded cartilage matrix. Extensive blunting of the notch (Fig. 7*b*) preceded the earliest signs of tearing at the root and propagation was accompanied by the formation of taut collagenous fibre bundles across it (Fig. 7*c*). Progressive inward movement of the radial notch occurred with further stressing of the slice. New fibrous material was exposed by fresh matrix rupture at the notch root with simultaneous fracture of those fibres furthest from the root (Fig. 7*d*). This primary tearing or rupture at the notch root was consistent with the intense concentration of stress immediately below the root (Fig. 7*d*).

The columns of chondrocytes previously aligned radially in the unloaded tissue acted as strain markers in the vicinity of the notch during loading. In the matrix below the root they contracted radially while to either side they underwent massive lateral shear.

The final stages of notch propagation involved the formation of a narrow neck of matrix (Fig. 7*e*), terminating either with the formation of a narrow array of fibres drawn out from the necked matrix (Fig. 7*f, g*) or abruptly by failure without any significant extraction of fibres from the final fracture surfaces (Fig. 8). The former mode of failure was observed only when the final loading of the slices was applied manually with great care.

In all the type A slices, except in the terminal stages of failure, the radial notch advanced in a stable manner. It was possible to interrupt loading and allow local yielding of tissue at the notch root to relieve the stress. Further advance of the notch would occur only with additional application of load.

Type B tissue. The increased stiffness of type B slices (Fig. 4) was consistent with the

* This phenomenon was assumed to resemble the photo-elastic effect exploited in experimental stress analysis.

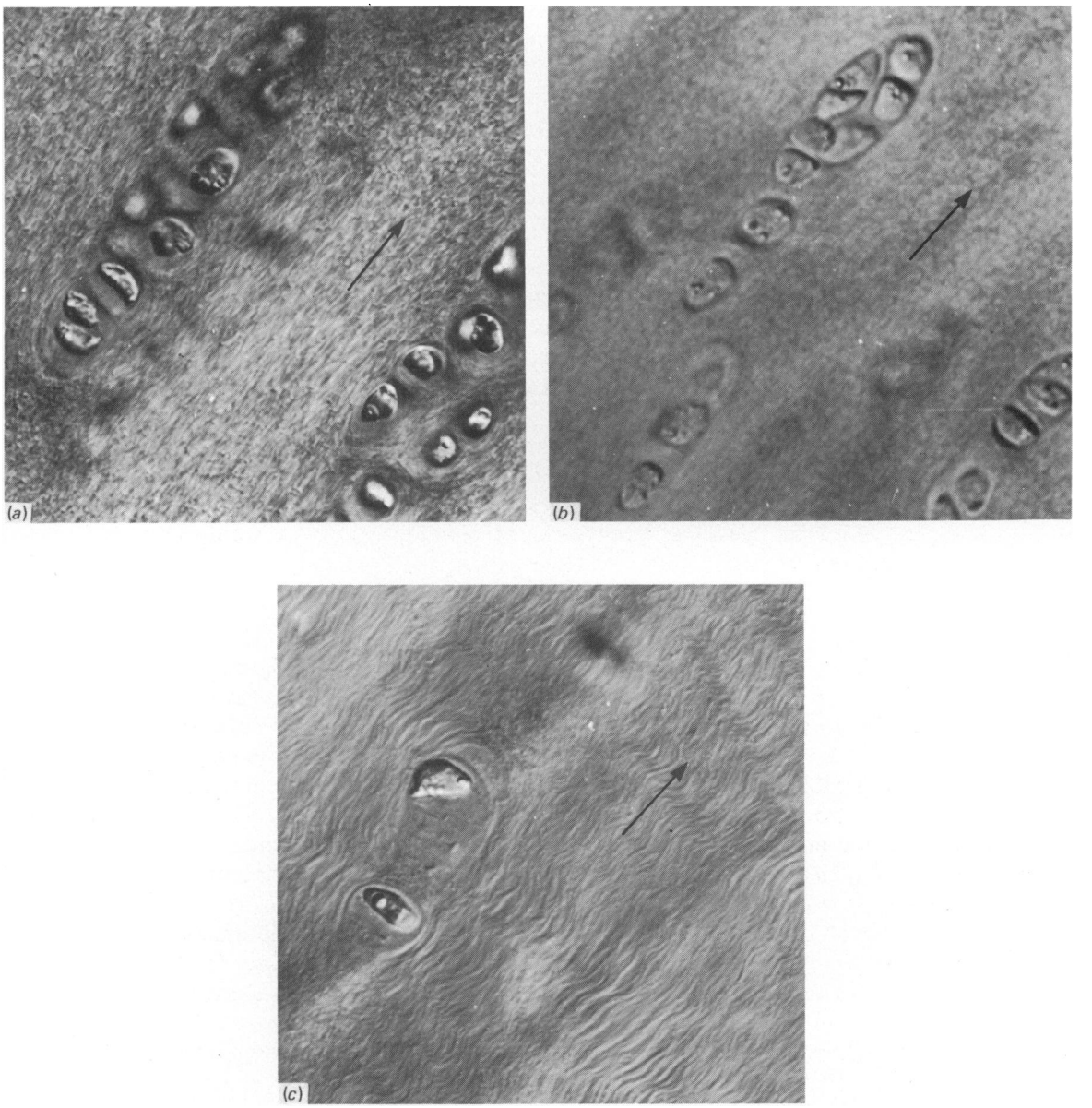

Fig. 6 (*a–c*). Deep zone structure of type A, B and C tissues in (*a–c*) respectively. Radial direction is indicated with an arrow in each Figure. × 530.

mode of propagation of the radial notch in this tissue. Following the onset of matrix rupture or tearing, the notch geometry was more acute than in the type A tissue with fibres spanning shorter distances above the notch root before fracturing (Fig. 9).

The concentration of stress below the notch was considerably less localised than in type A slices. This was apparent from the much wider band of contrast in the still intact matrix immediately below the notch root (Fig. 9*a*). The final stages of propagation involved little or no necking, indicating reduced distortion of the highly stressed matrix (Fig. 9*b*).

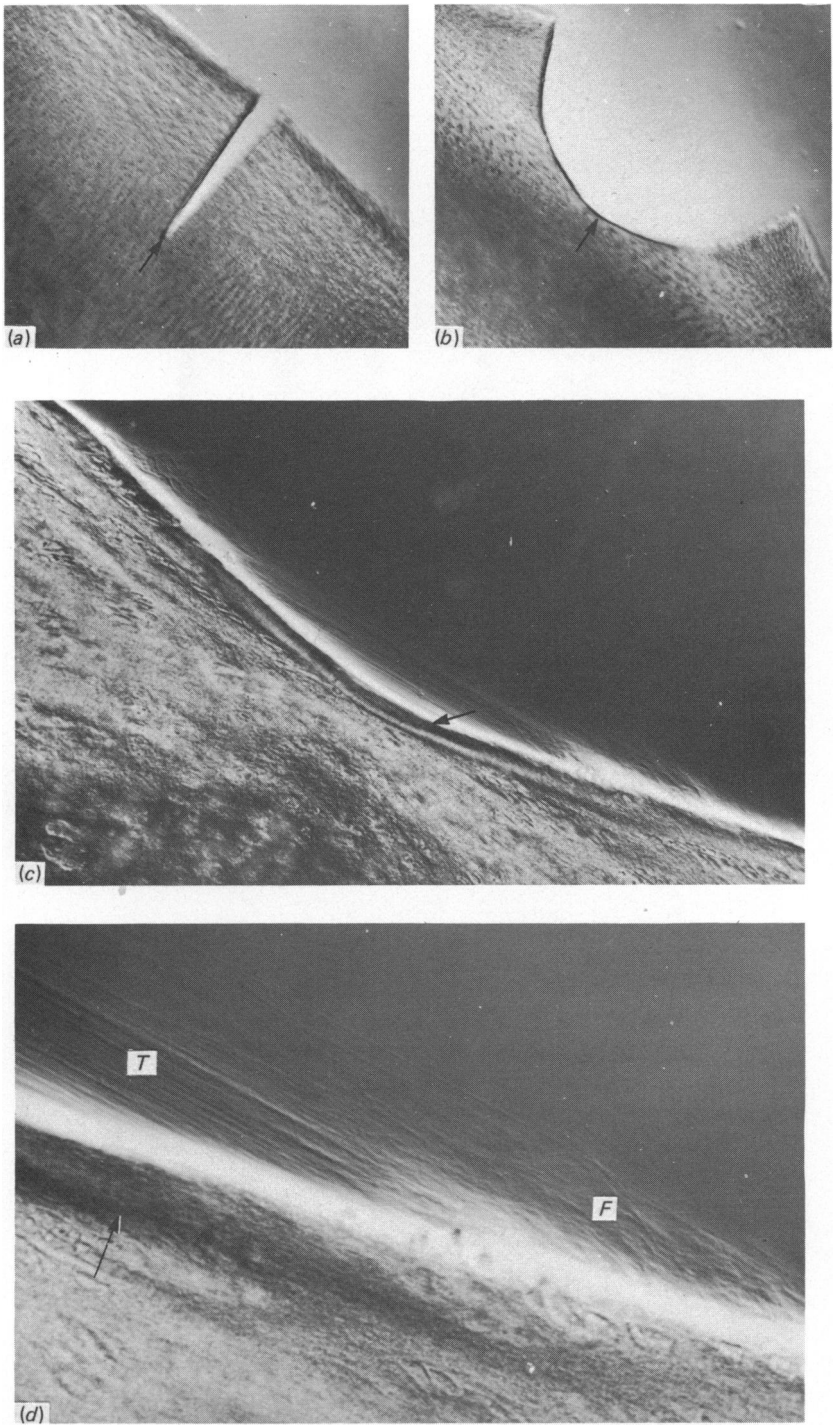

Fig. 7 (*a–g*). Sequence showing the propagation of a radial notch in a type A slice. (*a*) Zero load. Arrow indicates the notch root. × 42. (*b*) Slice loaded in tension up to onset of tearing at notch root (arrow). × 42. (*c*) Enlarged view of notch root in (*b*). Arrow indicates narrow stress band immediately below notch root. × 132. (*d*) Enlarged view of portion of (*c*) showing both taut fibres (*T*) and fractured fibres as indicated by their somewhat diffuse recoil (*F*). Arrow indicates darkened stress band. × 330. (*e*) Final stages of notch propagation through cartilage depth. × 132. (*f*) Neck of fibres drawn out from divided regions of matrix. × 132. (*g*) Fibrous array as in (*f*) but relaxed. × 132.

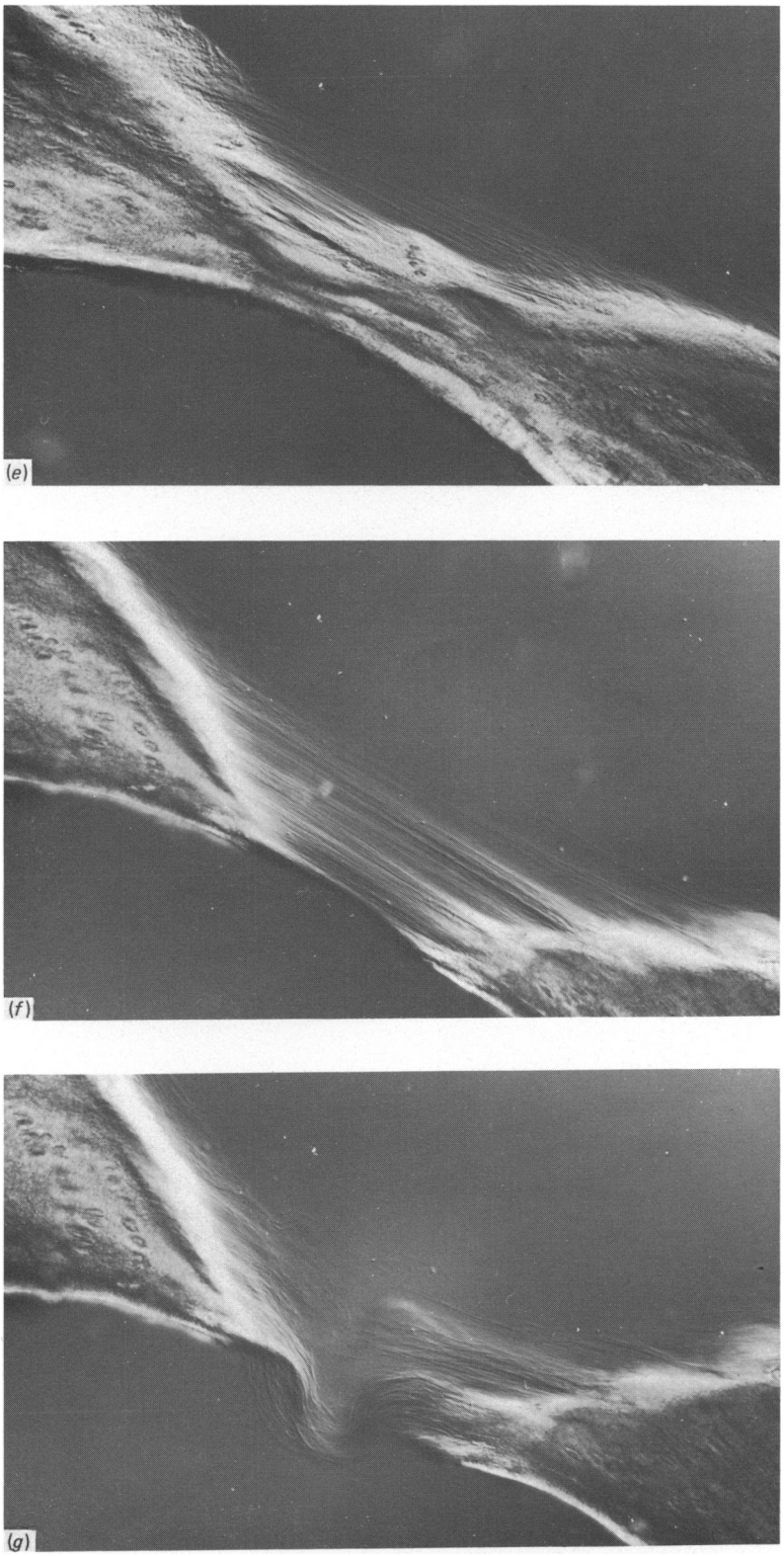

Fig. 7.

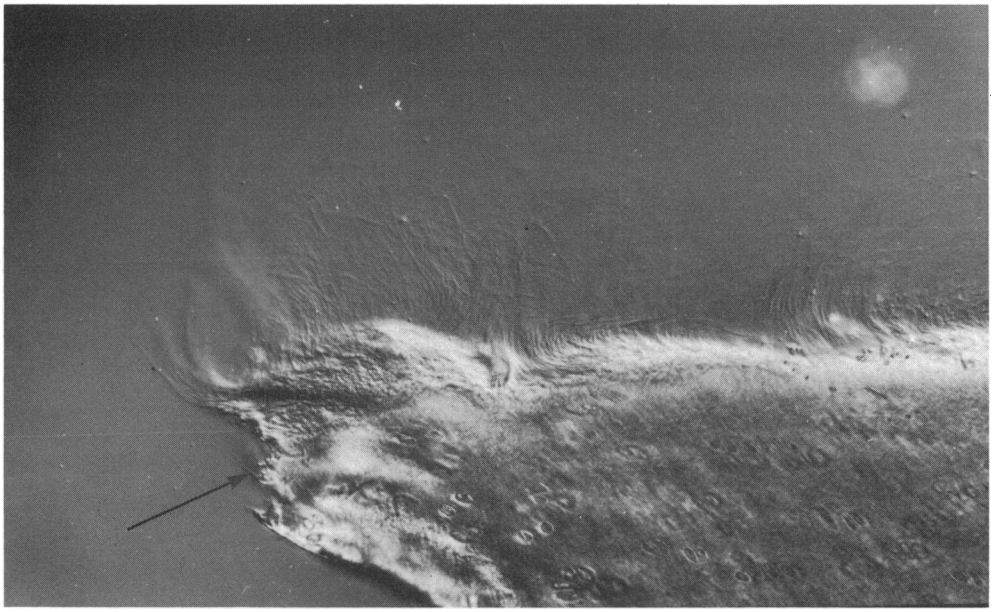

Fig. 8. Fractured half of type A slice in Fig. 7. The final stage of failure was abrupt and involved minimal fibre extraction (arrow). × 132.

In neither type A nor B slices was there any obvious increase in the rate of advance of the radial notch as it encountered the radial columns of chondrocytes typical of the deep zone.

Type C tissue. This tissue required only minimal loading (< 5 g) in tension to produce massive deformation of the matrix with stable propagation of the radial notch (Fig. 10). The flow of matrix below the notch was clearly delineated by the fan-like pattern of chondrocyte columns (Fig. 10*a*). There was little evidence of darkening due to stress at the notch root. Extensive neck formation (Fig. 10*b*) was accompanied by final fibre extraction (Fig. 10*c*), which sometimes occurred up to lengths of 2 mm or more.

Transverse notch propagation

Type A and type B slices. These slices responded to the transverse notch test in a similar manner apart from the different levels of loading at which propagation occurred (Fig. 4). The initial stages of loading of a transverse notch are shown in Figure 11. In both tissue types, it was impossible to propagate the notch in the transverse direction. The onset of matrix rupture was always accompanied by an immediate sideways or radial deflection of the notch either up towards the articular surface or down into the deep zone, or sometimes simultaneously in both directions (Fig. 11*c*) with one path eventually dominating. In all cases during this initial phase of tissue rupture, there was an intense concentration of stress in a narrow band at the notch root (Fig. 11*c*) with only minimal distortion of the matrix immediately beyond this root.

When this secondary tear path proceeded down through the deep zone, final failure of the slice occurred in a manner similar to that observed in the radially notched slices. However when an upward path was followed, the tear on approaching the

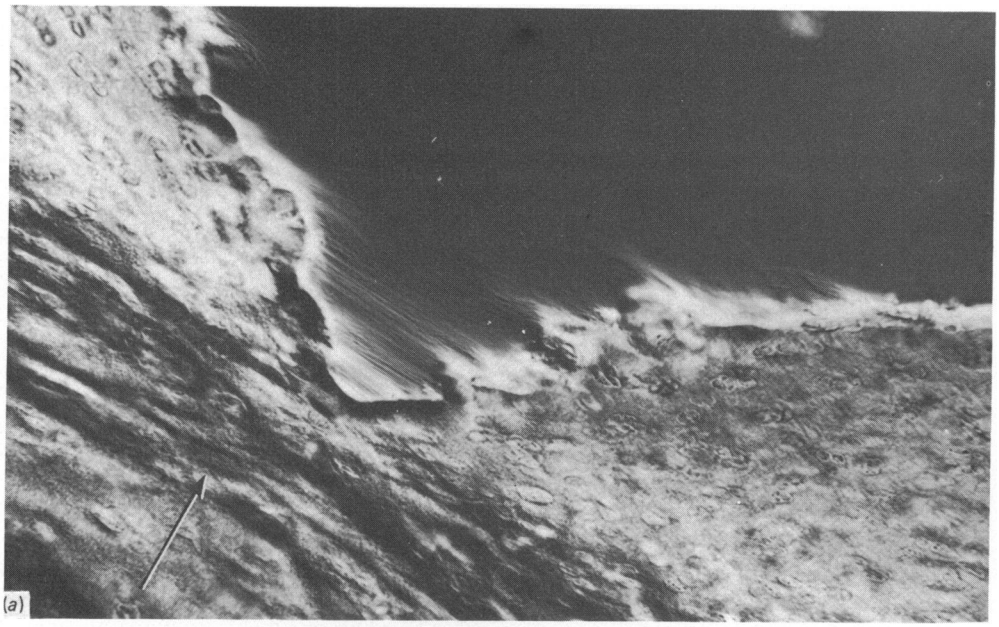

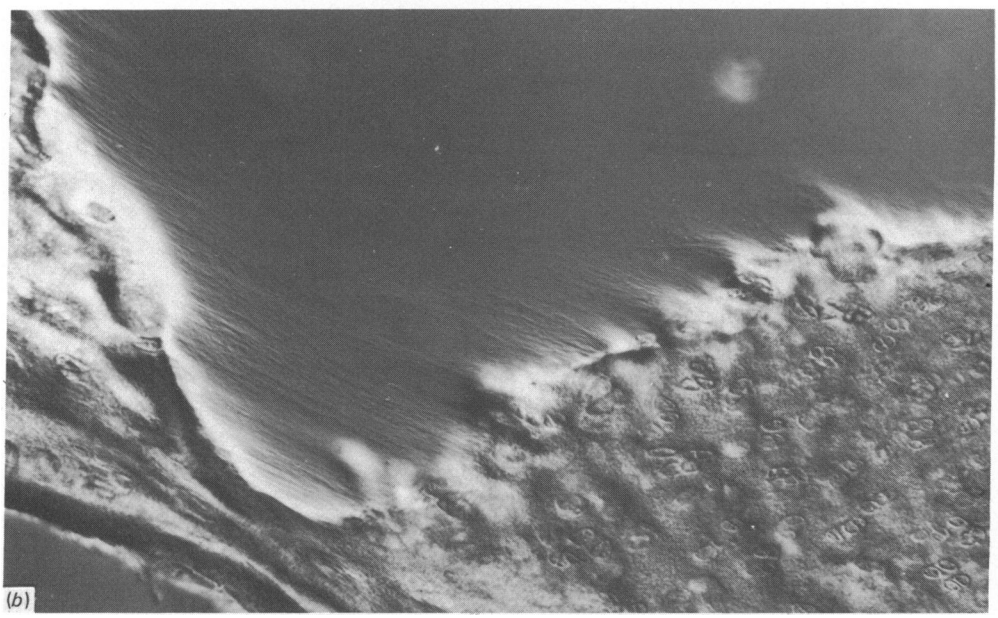

Fig. 9 (*a–b*). Radial notch propagating through a type B slice. (*a*) Note the acute geometry of the notch. Arrow indicates darkened stress band. (*b*) Final stages of propagation prior to fracture. × 128.

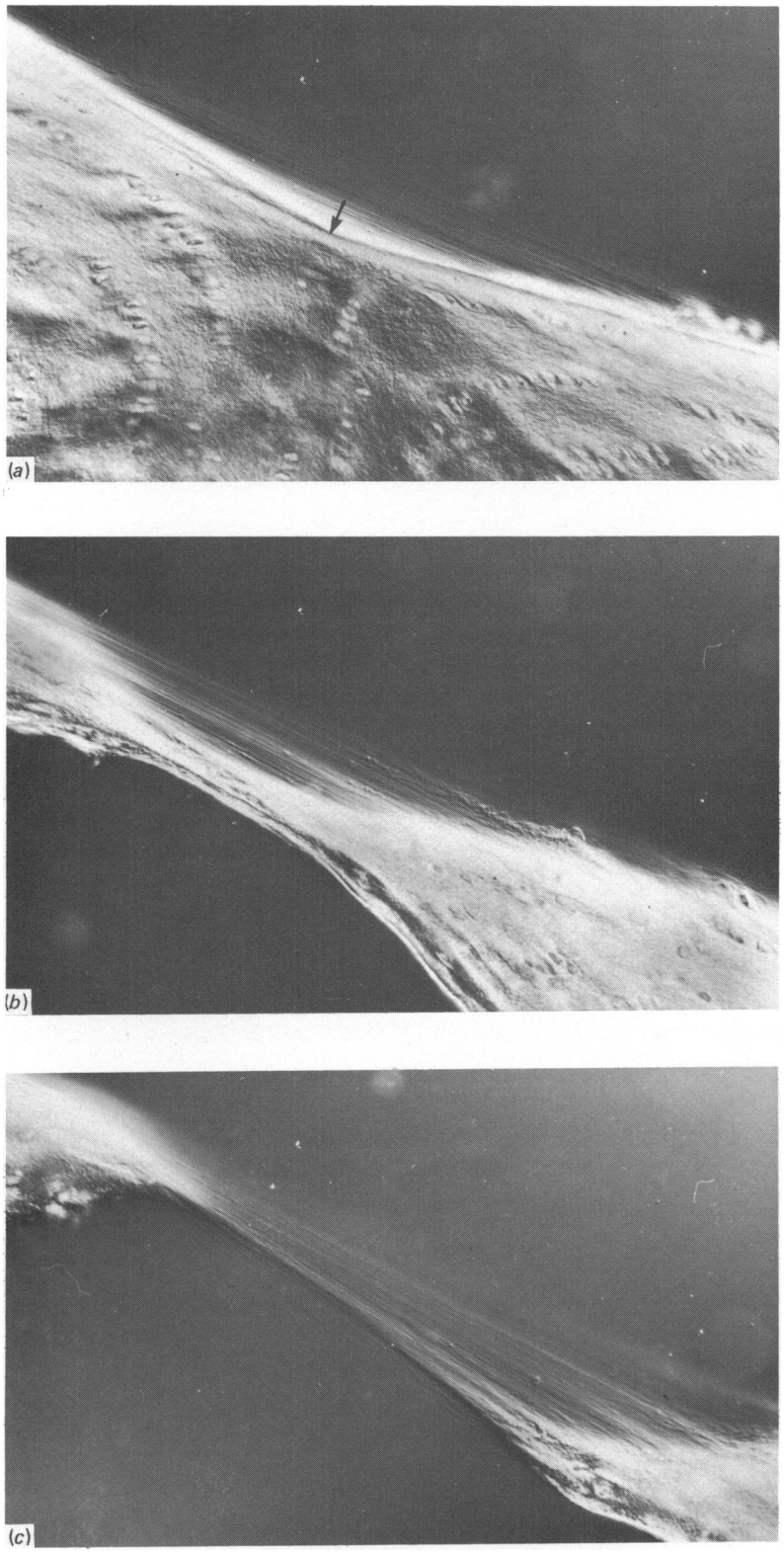

Fig. 10.

superficial zone was again deflected into a transverse plane, tracking parallel to but at a depth of about 150 μm below the articular surface. In effect, the final stages of failure involved a highly repeatable process of delamination of the entire superficial layer of cartilage (Fig. 11*d*). The partially re-assembled tissue resulting from the complex tear path followed by the original transverse notch is shown in Figure 11*e*.

Type C slices. Although this tissue, because of its extreme mechanical weakness, frequently failed prematurely at sites other than those initiated by transverse notching, the clearly resolved radial fibrous structure characteristic of the deep zone of this tissue (Fig. 6*c*) provided a direct view of the response of the matrix fibres to tension in the radial direction. The relaxed tissue at the transverse notch root exhibited a fine, partly crimped, fibrous structure lying parallel to the radial columns of chondrocytes (Fig. 12*a*). With very light loading, there was a visible tightening of this fibrous structure with minimal elongation radially (Fig. 12*b*). This limited extensibility of the matrix immediately below the transverse notch contrasted markedly with the extensive deformation observed with radial notching (Fig. 10).

DISCUSSION

An initial response to these experiments might be to question the validity of studies of essentially tensile stresses conducted on a biological tissue designed primarily to sustain compressive loads *in vivo*. It is, however, recognised that articular cartilage must derive its compressive load-bearing properties from complex interactions between the hydrated proteoglycans and the three dimensional collagen network. A direct compression experiment, even with simultaneous microscopical observation of the tissue response as has been previously performed, cannot yield insights into these interactions since only a generalised structural response is achieved. However, the present studies of structure and microtensile stresses when combined with selective pre-notching of the tissue permit a highly localised observation to be made of quite specific structural interactions within the various functional zones throughout the depth of the cartilage.

It is helpful to consider the present results in the context of the morphological model for articular cartilage proposed recently (Broom, 1982). In this model, the collagenous framework beneath the superficial zone is built up from a radial configuration of fibres. Imposed upon this arrangement at an ultrastructural level is a repeated short range change in direction of segments of each fibre along its length. With interlocking or crosslinking between such fibres the overall effect is to create a three dimensional meshwork from fibres which may in fact proceed continuously from the calcified cartilage radially up into the superficial layers. The degree of crosslinking will affect both the mechanical compliance and cartilage thickness (depending on the frequency and magnitude of these sideways segmental deflections) when this collagenous meshwork is packed out with hydrated proteoglycans.

In the author's view, the three types of cartilage discussed in the present paper represent three distinct levels of fibre crosslinking and hence different textural morphologies when viewed as fresh tissue under the optical interference microscope

---

Fig. 10 (*a–c*). Radial notch propagating through a type C slice. (*a*) Taut fibres span the notch root (arrow) and an extensive flow of matrix is indicated by distorted chondrocyte columns. × 132. (*b*) Final stages of matrix necking. × 132. (*c*) Extensive fibre extraction from matrix. × 132.

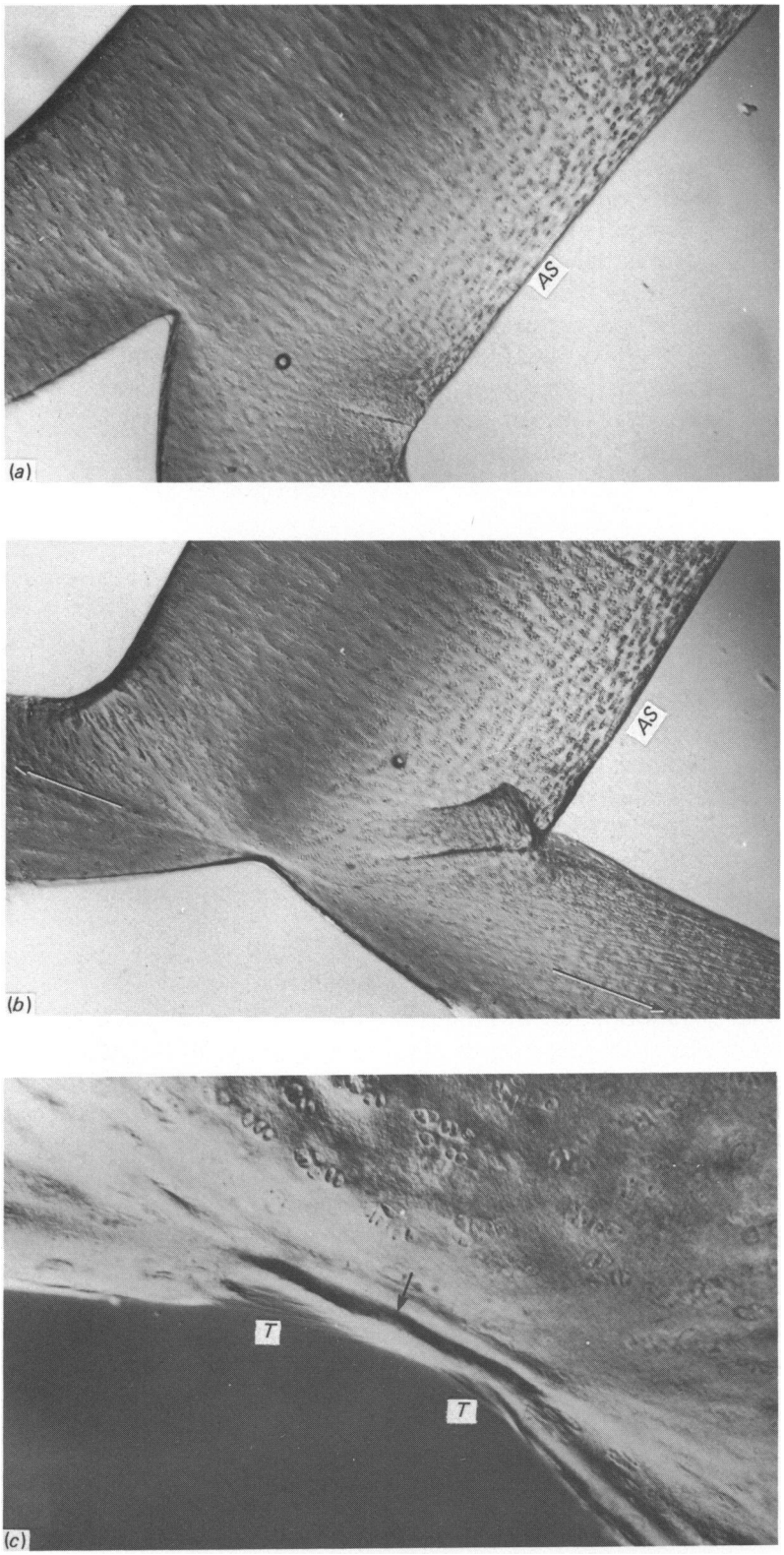

Fig. 11.

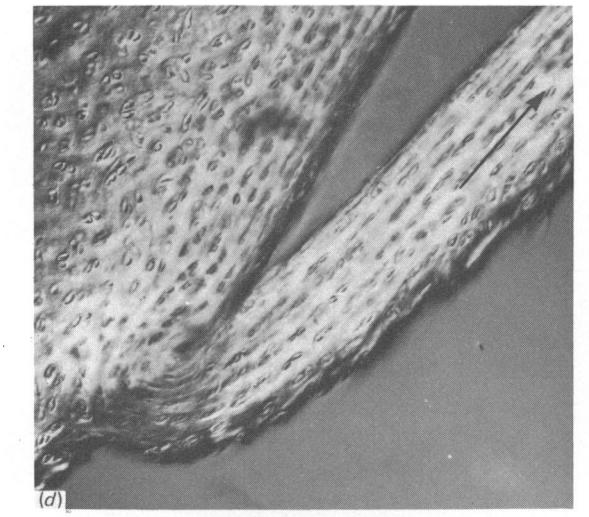

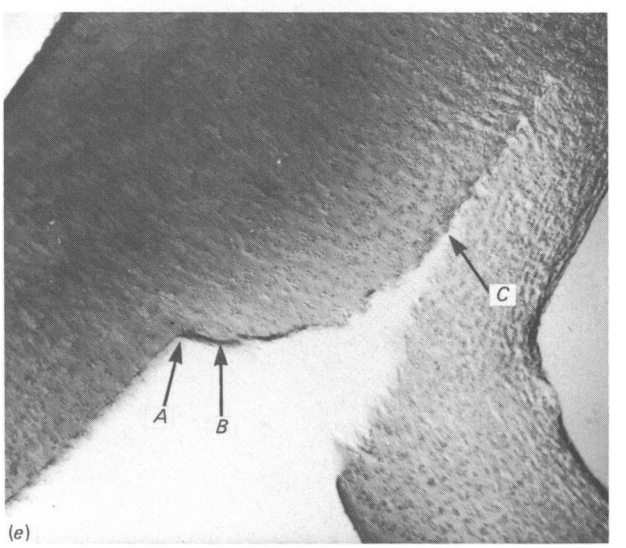

Fig. 11 (*a–e*). Loading of transverse notch in a type A slice. *AS*, articular surface. (*a*) Relaxed tissue. × 52. (*b*) Stressed to onset of tearing. Arrows indicate direction of loading. × 52. (*c*) Enlarged view of (*b*) showing two distinct sites of tearing (*T*, *T*). The narrow stress band is arrowed. × 136. (*d*) Delamination of the superficial layer. Arrow indicates direction of stripping. × 100. (*e*) Partially re-assembled slice following final delamination of superficial layer. *A*, original site of transverse notch, *B*, radial tear path, *C*, final delamination path. × 50.

(Fig. 6). Both types A and B reflect something of the range of morphologies and related mechanical properties characteristic of normal articular cartilage: a higher level of crosslinking resulting in a greater degree of fibre segment deflection away from a radial orientation would in turn yield a smaller thickness of less compliant articular cartilage corresponding to the uncurled type B category. The softened type C tissue is similar to that observed in the human tibial condyle where, in the central region exposed to direct femoral contact, degenerative changes occur from

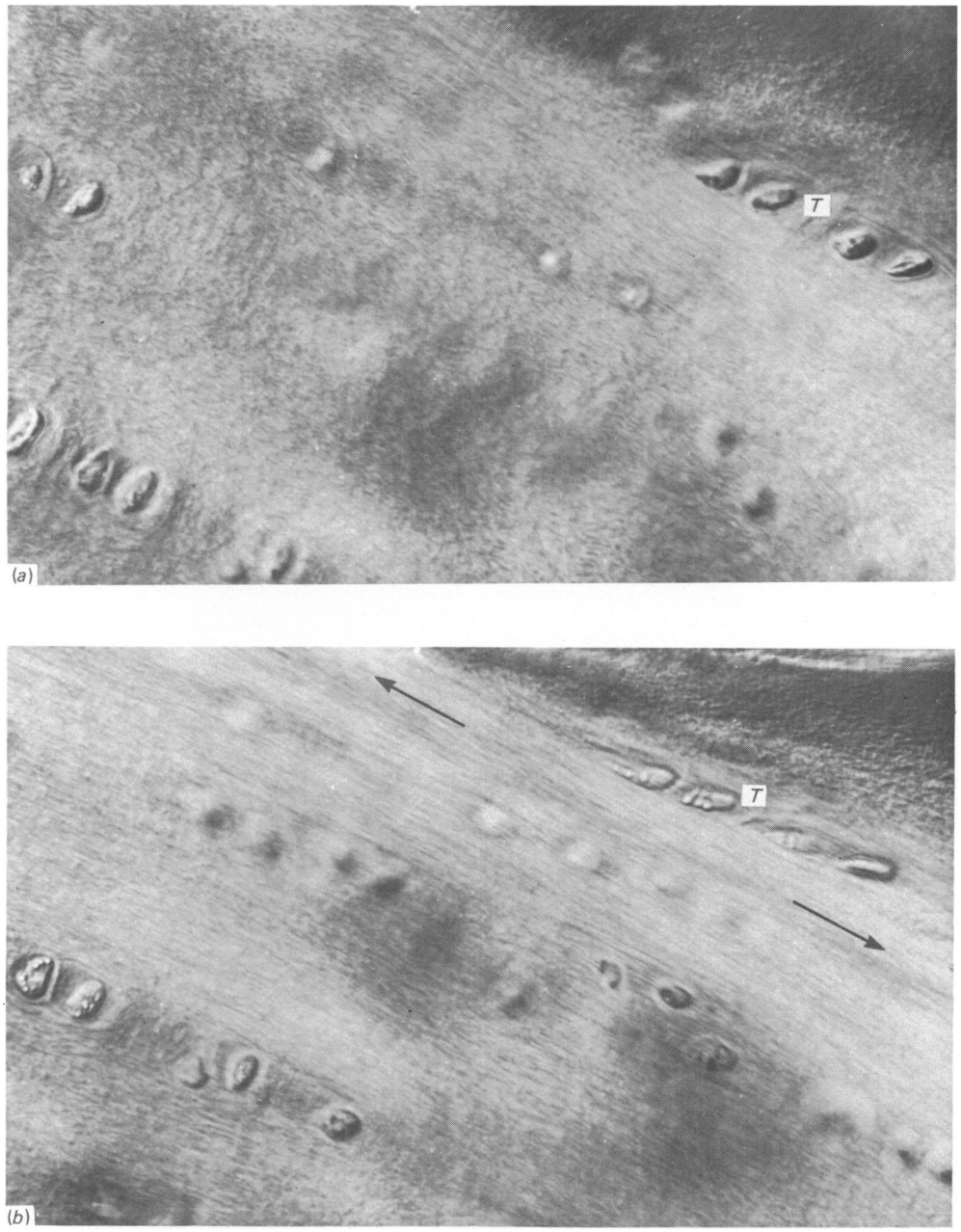

Fig. 12 (*a–b*). (*a*) Unloaded matrix structure at root of transverse notch in a type C slice. × 350. (*b*) Region as in (*a*) loaded. The same column of chondrocytes (*T*) is identified in each figure. Arrows indicate direction of loading. × 350.

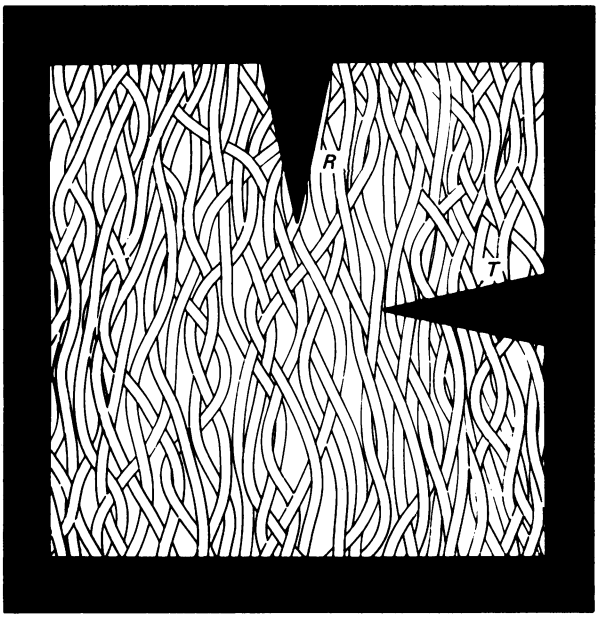

Fig. 13. Schematic diagram of radial (*R*) and transverse (*T*) notches and their probable relationship to the collagenous structure comprising the general matrix of articular cartilage.

early adult life onwards (Meachim, 1976; Santer, White & Roughley, 1981). It would reflect the opposite extreme, in which crosslinking is greatly reduced and the fibres largely revert to a pronounced radial configuration. This would yield a tissue of greatly increased compliance and radial thickness and in which the aggregates of parallel fibres are easily resolved with the light microscope.

In considering the response of cartilage to the notch experiment a comparison of radial versus transverse notch response provides substantial support for the morphological model summarised above. Propagation of a radial notch will involve principally the breaking of interfibre connections as well as the drawing out and eventual fracture of any fibres that are initially anchored in regions of matrix which have become divided by the advancing notch (Fig. 13). Conversely, the inability to propagate a transversely cut notch any further in the transverse direction is strong evidence for a primary radial arrangement of fibres in the deeper zone. Any direct advance of the transverse notch would involve the axial fracture of this entire array of fibres (Fig. 13). The stresses involved would be far in excess of those required to deflect the original transverse notch into a more radial path, as observed experimentally.

Further experimental confirmation of the morphological model is provided by the levels of matrix distortion and different patterns of stress concentration around the radial and transverse notches. In all three tissue types, there was minimum extension of the matrix at the root of the transverse notch as compared to the radial notch, indicating a marked 'strain–locking' effect. This effect is particularly evident in the soft type C tissue where the pronounced radial arrays of fibres are seen to tighten rapidly under the tension forces acting at the transverse notch root (Fig. 12). In the transversely notched type A and B slices, a marked concentration of stress always occurred in a narrow band at the notch root. This is consistent with the limited extension offered to the transverse notch root by the radial configuration of fibres.

Conversely with respect to the radial notch experiment when describing propagation principally in a direction parallel to the primary orientation of fibres, the model would, depending on the rigidity of the matrix (i.e. level of crosslinking), predict a variable amount of matrix distortion at the notch root as load is applied and the tissue commences to tear. This is in fact observed (Figs. 7, 9, 10).

There is little evidence from the radial notch experiments that the chondrocyte columns in the deep zone of normal cartilage represent planes of weakness along which the radial tear might preferentially propagate.

Radial notching demonstrates too the crucial role of the transversely aligned collagen fibres in the superficial layer in protecting the underlying matrix by means of a 'strain–locking' mechanism. Forces generated *in vivo* possibly by ploughing and shearing action are prevented from disrupting the matrix by the tension resisting membrane role of this superficial layer (Meachim & Stockwell, 1979).

Collagen fibres are known to extend less than 5% before fracture (Abrahams, 1967). However, the present study demonstrates that by controlling the rate of radial propagation varying levels of fibre extraction from the matrix could be achieved. The bonding relationship between an individual fibre and its surrounding matrix, however complex, is clearly time-dependent; rapidly applied extraction forces favour direct fracture of the collagen fibre rather than debonding with the matrix.

Two apparent inconsistencies exist in the load–extension data. Firstly, with respect to the radial notch in the normal tissue slices, the load required for propagation continues to increase even though the advancing notch progressively reduces the cross section of tissue available for load-bearing (Fig. 5). This can be explained by the presence of the intense band of stress in the matrix immediately below the radial notch root (Figs. 7, 9). The rheological properties of most soft connective tissues are highly non-linear with initial deformation involving only a small increase in stress (Fung, 1981). Therefore, with the radially notched slices, the matrix below the highly stressed band at the notch root, although deformed, will have sustained only a small fraction of the total load applied to the slice – the bulk of the load being sustained by the narrow band of matrix in the region of stress concentration. In theory, as rupture occurs at the root of the notch, its associated stress band will advance down through the cartilage matrix at approximately constant load. A possible explanation for this observed increase in load with increasing depth through the cartilage is that the fracture strength of the fibres and/or the strength of the fibre crosslinks also increase with depth.

The second anomaly concerns the higher level of loading required to propagate a primary radial notch in the deep zone compared to that for a transverse notch deflected radially within the deep zone (Fig. 5). Again, this is probably explicable in terms of the different pattern of loading on the radially notched slice compared to that in the tear region of the radially deflected transverse notch. The much greater opening strains imposed on the deflected tear by the geometry of the transversely notched slice would render it much more susceptible to propagation.

Finally, the consistent pattern of delamination observed in the superficial 150 μm layer of cartilage is clear evidence that a plane representing a major structural discontinuity exists parallel to and at this depth below the articular surface in bovine cartilage. Although becoming manifest as a zone of mechanical weakness in the experimental slices, this is probably an artefact of the sampling procedure and need not indicate the presence of a plane of weakness in the functioning cartilage. Such an artefact will arise as a result of the arrangement of fibres in the different zones

comprising the cartilage thickness. In the deeper zone where the primary radial arrangement includes only short range deflections of fibre segments away from the primary orientation, the slice thickness (0·1–0·2 mm) will have little influence on the measured mechanical strength, this being an accurate reflection of matrix biomechanical properties. If these radial fibres on approaching the articular surface retain their individual continuity but at some transition level turn sideways to form the tangential fibrous structure comprising the superficial layer, a distinct mechanical weakness will be observed in thin slices particularly in the zone of transition from radial to tangential orientation. Here in the thin slices the continuity of many of the fibres passing obliquely into the superficial layer will be abruptly terminated by the cut sides of the slice. Only those fibres which continue substantially into the superficial zone in the longitudinal dimension of the slice will provide adequate anchorage of the superficial zone to the underlying matrix. The observed pattern of delamination occurring consistently at a depth of approximately 150 μm is therefore in accord with a structural model embodying fibre continuity from the deeper matrix through to the superficial layer.

SUMMARY

A new experimental technique involving the observation of an artificial notch propagating through articular cartilage has been used to examine the biomechanical properties of this tissue. By predetermining both the orientation of the notch and its location with respect to the primary functional zones a more rigorous description of the structure/function relationships in cartilage has been achieved.

The principal findings are:

(1) A primary 'strain-locking' role for the superficial zone has been demonstrated experimentally in articular cartilage.

(2) Comparison of the behaviour of radial and transverse notches has revealed a primary structural anisotropy in the general matrix. This is strong evidence in support of the morphological model proposed in a recent paper by the present author.

(3) A range of mechanical responses is shown to be reflected consistently in structural features considered to arise principally from variations in the degree of crosslinking between the overall radial configuration of collagen fibres.

(4) It is possible to separate mechanically the collagen fibres from the general matrix and the bonding relationship between them is time-dependent.

(5) Measurement of loads required to propagate a radial notch suggest (*a*) that the strength of the fibres and/or that of the crosslinks between fibres increases with depth through the cartilage thickness, and (*b*) that the radial columns of chondrocytes typical of the deep zone do not represent planes of significantly reduced strength relative to the adjacent matrix.

(6) A major structural discontinuity exists in normal articular cartilage in a plane parallel to and below the articular surface. It is argued that this plane represents a major change in overall orientation of the collagen fibres.

Finally, by applying the experimental techniques described in this paper both to degenerative articular cartilage and to healthy articular cartilage in which the primary components have been selectively degraded enzymatically it should be possible to gain a more precise picture of the structural origin of malfunction in this tissue.

The author gratefully acknowledges the support of the Medical Research Council of New Zealand in the form of a Senior Research Fellowship. The technical assistance of D. L. Marra of the School of Engineering, University of Auckland, is also acknowledged.

REFERENCES

ABRAHAMS, M. (1967). Mechanical behaviour of tendon *in vitro*. *Medical and Biological Engineering* **5**, 433–443.

BROOM, N. D. (1978). Simultaneous morphological and stress–strain studies of the fibrous components in wet heart valve leaflet tissue. *Connective Tissue Research* **6**, 37–50.

BROOM, N. D. (1982). Abnormal softening in articular cartilage: its relation to the collagen framework. *Arthritis and Rheumatism* **25**, 1209–1216.

BROOM, N. D. & MYERS, D. B. (1980). A study of the structural response of wet hyaline cartilage to various loading situations. *Connective Tissue Research* **7**, 227–238.

BROOM, N. D. & POOLE, C. A. (1982). A functional–morphological study of the tidemark region of articular cartilage maintained in a non-viable physiological condition. *Journal of Anatomy* **135**, 65–82.

BROOM, N. D. & POOLE, C. A. (1983). Articular cartilage collagen and proteoglycans: their functional interdependency. *Arthritis and Rheumatism* **26**, 1111–1119.

FRY, H. (1974). Interlocked stresses in articular cartilage. *British Journal of Plastic Surgery* **27**, 363.

FUNG, Y. C. (1981). *Biomechanics – Mechanical Properties of Living Tissue*, Ch. 7. New York: Springer-Verlag.

MEACHIM, G. (1976). Cartilage fibrillation on the lateral tibial plateau in Liverpool necropsies. *Journal of Anatomy* **121**, 97–106.

MEACHIM, G. & STOCKWELL, R. A. (1979). The matrix. In *Adult Articular Cartilage*, 2nd ed. (ed. M. A. R. Freeman), pp. 1–67. London: Pitman Medical.

PHILLIPS, V. A. (1971). *Modern Metallographic Techniques and Their Applications*, p. 83. New York: Wiley Interscience.

SANTER, V., WHITE, R. J. & ROUGHLEY, P. J. (1981). Proteoglycans from normal and degenerate cartilage of the adult human tibial plateau. *Arthritis and Rheumatism* **24**, 691–700.

WEIGHTMAN, B. & KEMPSON, G. E. (1979). Load carriage. In *Adult Articular Cartilage*, 2nd ed. (ed. M. A. R. Freeman), pp. 291–331. London: Pitman Medical.